Acta. Chim. Asiana., 2023, 6(2), 328 – 337
e-ISSN/p-ISSN 2550-0503/2550-049x
Available online at: www.aca.unram.ac.id

RESEARCH PAPER

Increasing corrosion resistance of binary Al-Alloy through implanting with some transition elements and heteroatom organic compounds

Fatemeh Mollaamin[1,2]

[1]Department of Food Engineering, Faculty of Engineering and Architecture, Kastamonu University, Kastamonu, Turkey
[2]Department of Biology, Faculty of Science, Kastamonu University, Kastamonu, Turkey

DOIs: 10.29303/aca.v6i2.166

Article info:

Received 04/05/2023

Revised 18/06/2023

Accepted 18/05/2023

Available online 23`/06/2023

Abstract: Decorating of Transition metals (TMs) on the "AlMg" nanoalloy has been studied on the basis of Langmuir adsorption applying "ONIOM" model with three levels of «high, medium and low» by using "LANL2DZ /6-31+G(d,p)/EPR-III", "semi-empirical" and "MM2" functions. The fluctuation of "NQR" has estimated the inhibiting role of pyridine and alkylpyridines containing 2-picoline (2Pic), 3-picoline (3Pic) ,4-picoline (4Pic), and 2,4-lutidine (24Lut) for (Sc, Ti, Cr, Ni, Cu, Zn)-doped AlMg alloy nanosheet due to "N" atom in the benzene cycle of heterocyclic carbenes being near the monolayer surface of ternary "TM–(Al–Mg)" (TM= Sc, Ti, Cr, Ni, Cu, Zn) nanoalloys. The "NMR" spectroscopy has remarked In fact, the NMR results of the adsorption of pyridine and alkylpyridines of 2Pic, 3Pic, 4Pic and 24Lut molecules represent spin polarization on the TM (Sc, Ti, Cr, Ni, Cu, Zn)-doped Al–Mg nanoalloy surfaces that these surfaces can be employed as the magnetic N-heterocyclic carbene sensors. In fact, "TM" sites in "TM–(Al–Mg)" nanoalloy surfaces have bigger interaction energy amount from "Van der Waals' forces" with pyridine and its nitrogen heterocyclic family that might cause them large stable towards coating data on the nanosurface. It has been estimated that the criterion for choosing the surface linkage of "N" atom in pyridine and alkylpyridines in adsorption sites can be impacted by the existence of close atoms of aluminum and magnesium in the "TM–(AlMg)" surfaces. Moreover, "IR" spectroscopy has exhibited that (Sc, Ti, Cr, Ni, Cu, Zn)-doped AlMg alloy nanosheet with the fluctuation in the frequency of intra-atomic interaction leads us to the most considerable influence in the vicinage elements generated due to inter-atomic interaction. Comparison to 〖∆G〗_ads^o amounts versus dipole moment has illustrated a proper accord among measured parameters based on the rightness of the chosen isotherm for the adsorption steps of the formation of Py@Sc–(Al–Mg), Py@Ti–(Al–Mg), Py@Cr–(Al–Mg), Py@Ni–(Al–Mg), Py@Cu–(Al–Mg), and Py@Zn-(Al–Mg) complexes. Thus, the interval between nitrogen atom in pyridine during interaction with transition metals of "Sc, Ti, Cr, Ni, Cu, Zn" in "TM–(Al–Mg)" nanoalloys, (N→TM), has been estimated with relation coefficient of R^2 = 0.9284. Thus, the present has exhibit the influence of "TMs" doped on the "Al–Mg" surface for adsorption of N-heterocyclic carbenes of pyridine and alkylpyridines by using theoretical methods.

Keywords: NHCs@TM–(Al–Mg); Sc; Ti; Cr; Ni; Cu; Z; Langmuir adsorption; N-heterocyclic carbenes; pyridine; alkylpyridines; CAM-B3LYP/EPR-III,LANL2DZ,6-31+G(d,p); DFT; ONIOM

Citation: Mollaamin, F. (2023). Increasing corrosion resistance of binary Al-Alloy through implanting with some transition elements and heteroatom organic compounds. Acta Chimica Asiana, 6(2), 327–342. https://doi.org/10.29303/aca.v6i2.166

INTRODUCTION

Heterocyclic carbenes containing "N" atoms are impressible corrosion compounds for diverse series of metals in varied acidic solutions [1-8]. Since various specifications of heterocycles carbenes are remarked, it is crucial that the electrons of a series of heterocycles are considered [9-16]. Thus, functionalized heterocycles as corrosion inhibiting agents have been selected and identified based on their physico-chemical specifications, and an attention has been assigned to the quantitative assessment of the internal and steric impact of these structures upon their inhibiting output [17-22]. It has been seen that heterocycles containing "N" atoms are appropriate corrosion inhibiting agents for most of metal crystals in diverse acidic conditions; For example benzotriazole at the "Cu" and "Fe" electrode, isoquinoline and imidazole families at the "Fe" electrode are impressive inhibiting agents for corrosion of these metal crystals [23-39]. The microscopic interaction and reaction mechanism between molecules might be deeply revealed from the quantum chemical specifications which provide a advantageous track to detect adsorption tendency between molecules and interfaces at the atomic and molecular stages [40-42]. Nowadays, it has been shown that pyridine and alkylpyridines had been employed as corrosion inhibiting agents of the "Al" crystal. There are many investigations that have been devoted to the usage of potent heterocycles and heteroatomic molecules consisting of organic materials that enhance the anticorrosion qualifications of metal surfaces and alloys. The presence of heteroatoms containing "O, S, N, P" atoms, "aromatic rings" and "multiple bonds" with "π-electrons" in these inhibiting agents support largely the foundation of inactive blocks on metal crystal and alloys [43-48]. Moreover, it has been analyzed that alkylpyridines have been widely used through their strong polarity which enhances in ionic liquids and solution media. There is a reasonable connection between the thickness of the passive layer and the effectiveness of inhibiting the corrosion action [49-51].

In the previous works, the adsorption analysis of pyridine, and nitrogen heterocyclic derivatives onto pristine two-layer aluminum surface [52], pure monolayer aluminum metal surface based on Freundlich Adsorption [53] have been investigated. Furthermore, the data of Langmuir adsorption model of organic inhibitors containing pyridine and alkylpyridines [54]; benzotriazole, 8- hydroxyquinoline, and 2-mercaptobenzothiazole (2-MBT) [55] by using monolayer binary alloys of the "AlMg", "AlGa", "AlSi" surfaces have been reported .Besides, the role of pyridine and its family compounds as corrosion inhibiting agents for monolayer ternary "Al" nanoalloys including "AlMgSi", "AlMgGe", "AlMgSn" surfaces have been studied [56].

Now, the present work intends to extend the previous works [52-56] toward the investigation of transition metals doped on the "Al–Mg" surface for adsorption of N-heterocyclic carbenes of pyridine and alkylpyridines consisting of «2-picoline (2Pic), 3-picoline (3Pic),4-picoline (4Pic), and 2,4-lutidine (24Lut)» by using through "CAM-B3LYP/EPR-III, LANL2DZ,6-31+G(d,p)" theoretical methods.

MATERIALS AND METHODS

TM-doped AlMg alloy & corrosion resistance

"Al-alloys" might be sensitive to intergranular corrosion process if "second-phase" micro components are generated at grain boundary orientations. A corrosion ability of the alloy is separate from that of the matrix will also make intergranular corrosion process. The existence of perceptible values of soluble alloying elements like "Cu, Mg, Si, and Zn" will cause these alloys sensitive to "stress-corrosion" cracking process [57-59]. Certain elements like Cu and Mg added to Al alloys ameliorate the mechanical attributes and conduct the alloy to reply the heat dealing. The existence of magnesium also increases resistance and reduces the rate of strength loss at high temperature in the alloys.

Aluminum-magnesium "AlMg" alloys are lighter than other "Al-alloys" and much less flammable than other alloys consisting of high values of "Mg" which can be doped with some transition metal elements including "Sc, Ti, Cr, Ni, Cu, Zn" (Figure1). The great augmenting in persistence at raised temperature has been done after solution manner through activating settlement making hard due to "Mg" having phases.

Material"ONIOM" approach

Based on this research, "ONIOM" methodology, "QM" has been performed due to the "DFT" methodology of "CAM-B3LYP" with "6-31+G(d,p) " basis set for "C" and "H" atoms , EPR-III for "N" atom and "LANL2DZ" for the transition metals of "Sc, Ti, Cr, Ni, Cu, Zn" atoms in the adsorption sites. "QM2" has been fulfilled on certain "Al" and "Mg" atoms in the adsorption sites due to semi-empirical force fields. And, a "QM3" has been discussed on the other "Al" and "Mg" atoms with "MM2" methodology (Figure 2) [85-60].

"ONIOM" as a "three-layered" methodology of authorizes us to unravel a bigger system more explicitly than the "one-layered" model which may behave a medium size system stringently like a huge system with usual exactitude (Figure2) [63]. So, The mentioned "three-layered" sample has been used to activate barriers for the (Py, 2Pic, 3Pic, 4Pic and 24Lut) onto mono-layer TM–(AlMg) (TM= Sc, Ti, Cr, Ni, Cu, Zn) alloy surfaces towards generating the "Langmuir adsorption" complexes consisting of Py@TM–(AlMg), 2Pic@TM–(AlMg), 3Pic @TM–(AlMg), 4Pic@TM–(AlMg), and 24Lut @TM–(AlMg) (Figure2).

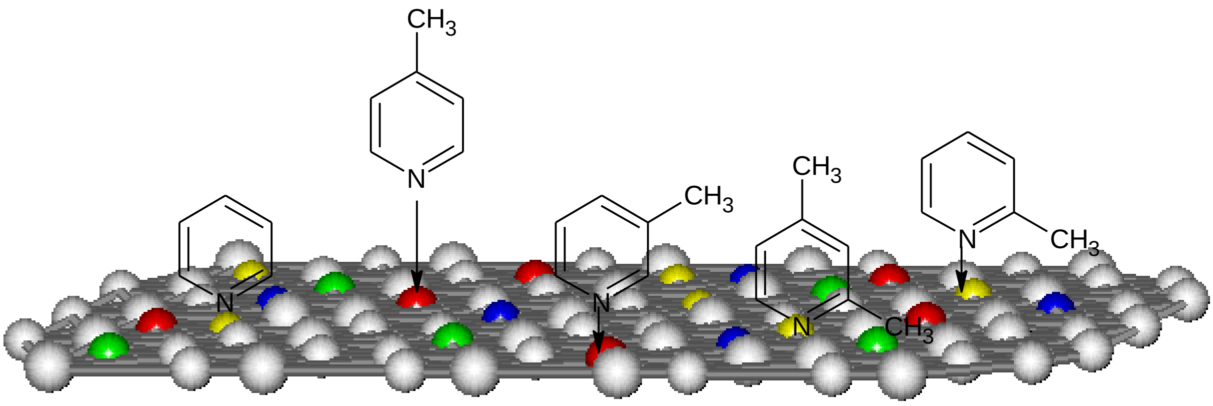

Figure1. Langmuir adsorption of N–containing carbenes on the (Sc, Ti, Cr, Ni, Cu, Zn)–doped aluminum–magnesium nanosheet alloy

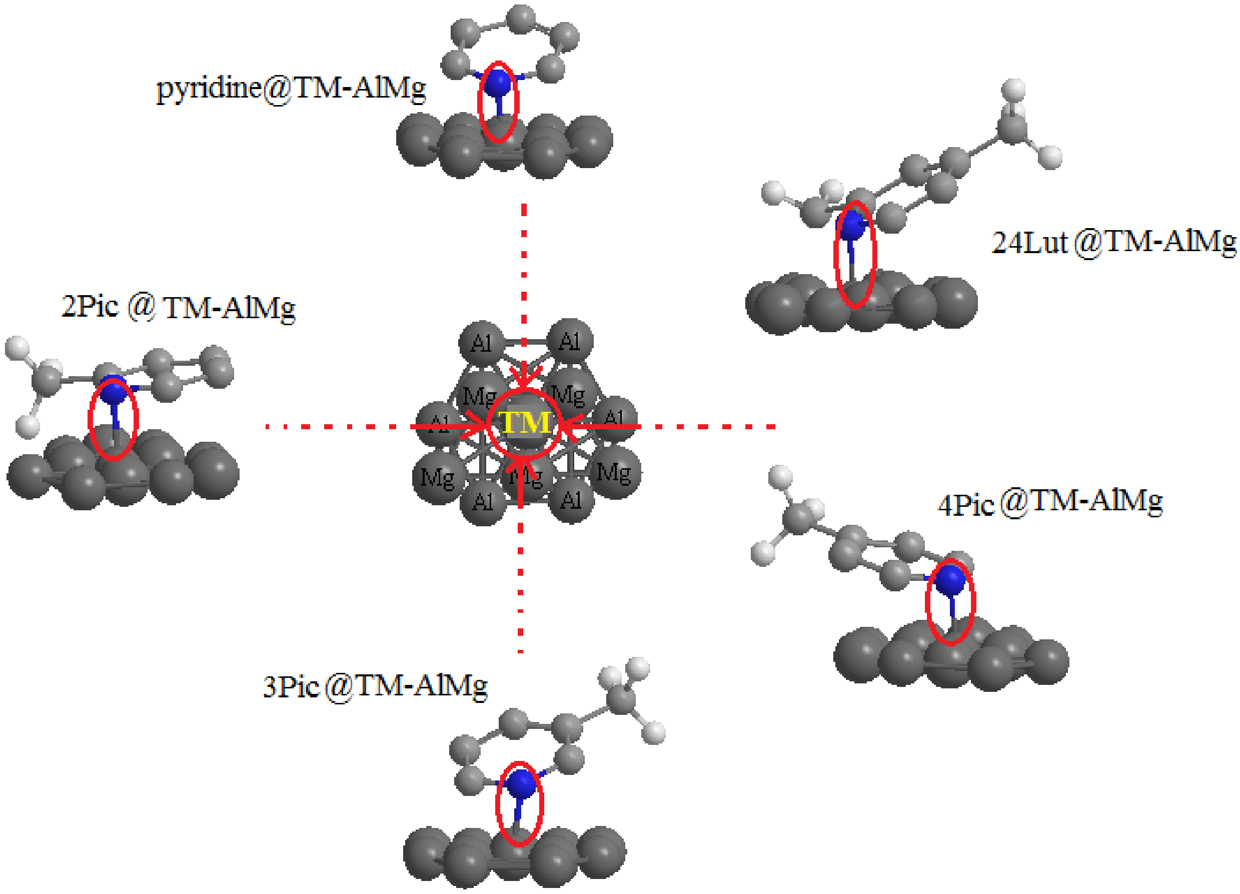

Figure2. Adsorbing N-heterocyclic carbenes (NHCs) of pyridine and alkylpyridines (2Pic, 3Pic, 4Pic and 24Lut) onto TM–(Al–Mg) alloy surfaces (TM= Sc, Ti, Cr, Ni, Cu, Zn) in various surfaces of "high", "medium" and "low" levels of "ONIOM" methodology.

"DFT" Method

"Hohenberg-Kohn" (HK) functions have rigidly made the electronic density permissible as fundamental variable to electronic and structure computations. In other words, developement of the applied "DFT" methodology only became notable after "W. Kohn and L. J. Sham" released their reputable series of equations which are introduced as "Kohn-Sham" (KS) equations [25,26]. Considering the electronic density within the "KS" image directs us to a remarkable reduction of the quantum computing. Thus, the "KS" methodology lightens the route for

Acta. Chim. Asiana., 2023, 6(2), 328 – 342

pursuing the systems that cannot be discussed by conventional "ab-initio" methodologies. "Kohn and Sham" introduce the solution which brings up the "mono-electronic orbitals" to account the kinetic energy in a simple and relatively exact, by founding a residual modification that might be computed apart [64-73].

"DFT" or "Density functional theory" calculations have been accomplished by using "Gaussian 16 revision C.01" program package [74]. The input Z-matrix for the N-heterocyclic carbenes "NHCs" of pyridine and alkylpyridines as corrosion inhibiting agents adsorbed onto the "TM–(AlMg)" alloy surfaces "(TM= Sc, Ti, Cr, Ni, Cu, Zn)" (Figures 1&2) have been provided with "GaussView 6.1" [75] due to the rigid system and coordination format of which a blank line has been cited and using "LANL2DZ,EPR-III, 6-31+G(d,p)" basis sets to distinguish "chemical shielding", "frequencies", "thermodynamic properties", "electrostatic and electronic potential", "natural atomic charges, "projected density of state" and other quantum properties for this work. The rigid "PES" has been calculated at "CAM-B3LYP/EPR-III,LANL2DZ,6-31+G(d,p)" for pyridine and alkylpyridines (2Pic, 3Pic, 4Pic and 24Lut) adsorbed onto "TM–(AlMg)" alloys surfaces "(TM= Sc, Ti, Cr, Ni, Cu, Zn)" in which the small energy difference between the formations of "NHCs@ TM–(AlMg)" complexes can direct us to an efficient coated crystal for preventing the corrosion process. Thus, it has been discovered that the crystal binding site preferable of "N-atom" is largely impacted by the essence of neighboring "N" atoms. The calculated "NHCs@ TM–(AlMg)" pair repartition functions have exhibited that the formation of crystals addresses to shorter "Nitrogen→TM–alloy" bond lengths when it is figured out to the analogous growth (Figures 1&2).

RESULTS AND DISCUSSION

The adsorption of pyridine and alkylpyridines as N–heterocyclic carbenes on the "Al–Mg" Nanoalloy doped with Transition Metals "(Sc, Ti, Cr, Ni, Cu, Zn)" in "NaCl" solution was allocated by the most appropriate "Langmuir isotherm", which remarks the "chemisorptive" nature of the bond among the "NHCs@TM–(Al–Mg)" complexes, the equilibrium distribution of ions of the adsorbing compound between the solid and liquid phases, and a monolayer attribute. The adsorbed molecules are kept on the "TM–(Al–Mg)" surface with chemisorbed inhibitors having high protection (Figure2).

Electronic structure

Figure3 (a-f) shows the projected density of state "PDOS" of the Transition Metals (Sc, Ti, Cr, Ni, Cu, Zn) decorated Al–Mg surface. The appearance of the energy states (d-orbital) of "Sc, Ti, Cr, Ni, Cu, Zn" within the gap of Al–Mg surface induces the reactivity of the system. It is clear from the figure that after doping with "TM" atoms and there is a significant contribution of "TM" d-orbital in the unoccupied level. Based on the population analysis and "DOS" it can be concluded that "TM" remains in the cationic state and it can accept more electrons from other atoms. Therefore, the curve of partial "DOS (PDOS)" has described that the "p states" of the adsorbing process of "N" atom on the "TM–(Al–Mg)" surface are overcoming due to the conduction band (Figure3a-f). A distinguished metallic trait might be seen in "TM–(Al–Mg)" crystal because of the potent interaction between the "p states" of "Al", "Mg" and the "d" state of "TM" near the "Fermi energy". Furthermore, the essence of covalent traits for these clusters has displayed the similar energy value and image of the "PDOS" for the "p orbitals" of "Al", "Mg Figure3(a,b,c) shows that the Sc–(Al–Mg), Ti–(Al–Mg) and Cr–(Al–Mg) states, respectively, have the most contribution at the middle of the conduction band between -5ev to -10ev, while contribution of aluminum and magnesium states are enlarged and similar together, but scandium, titanium and chromium states have little contributions.

Figure3(d,e,f) indicates that the Ni–(Al–Mg), Cu–(Al–Mg) and Zn–(Al–Mg) states, respectively, have more contribution at the middle of the conduction band between -5ev to -10ev, while contribution of aluminum and magnesium states are limited, but nickel, copper and zinc states have major and expanded contributions. "and "d orbitals" of "TM" (Figure3a-f).

Atomic charge & Magnetism properties

Nuclear magnetic resonance spectrums of TM–doped "Al–Mg" alloy surface as the potent sensor for adsorbing the N-heterocycles of pyridine and alkylpyridines can unravel the indicated transition metals of "Sc, Ti, Cr, Ni, Cu, Zn" in the active site of "AlMg" alloy surface through the formation of the covalent binding between N-heterocyclic carbenes (adsorbate) and surface (adsorbent). The chemical shielding extracts from "Nuclear magnetic resonance" or "NMR" can be applied for allocating the structural and geometrical specifications of materials. As a matter of fact, "Gauge Invariant Atomic Orbital" or "GIAO" methodology has been recommended as a valid methodology for "NMR" parameter computations and "ONIOM" has caught much regards for gaining "NMR" chemical shielding of "inhibitor-surface" complexes such as isotropic and anisotropic chemical shielding tensors [76].

The "NMR" data of isotropic "σiso" , anisotropic shielding tensor "σaniso" and Bader charge "Q" of

Acta. Chim. Asiana., 2023, 6(2), 328 – 342

transition metals attached for Py@TM–(Al–Mg), 2Pic→@TM–(Al–Mg), 3Pic@TM–(Al–Mg), 4Pic@TM–(Al–Mg), and 24Lut@ TM–(Al–Mg) [TM= Sc, Ti, Cr, Ni, Cu, Zn] have been computed by "Gaussian 16 revision C.01" program package [74] and been shown in Table1.

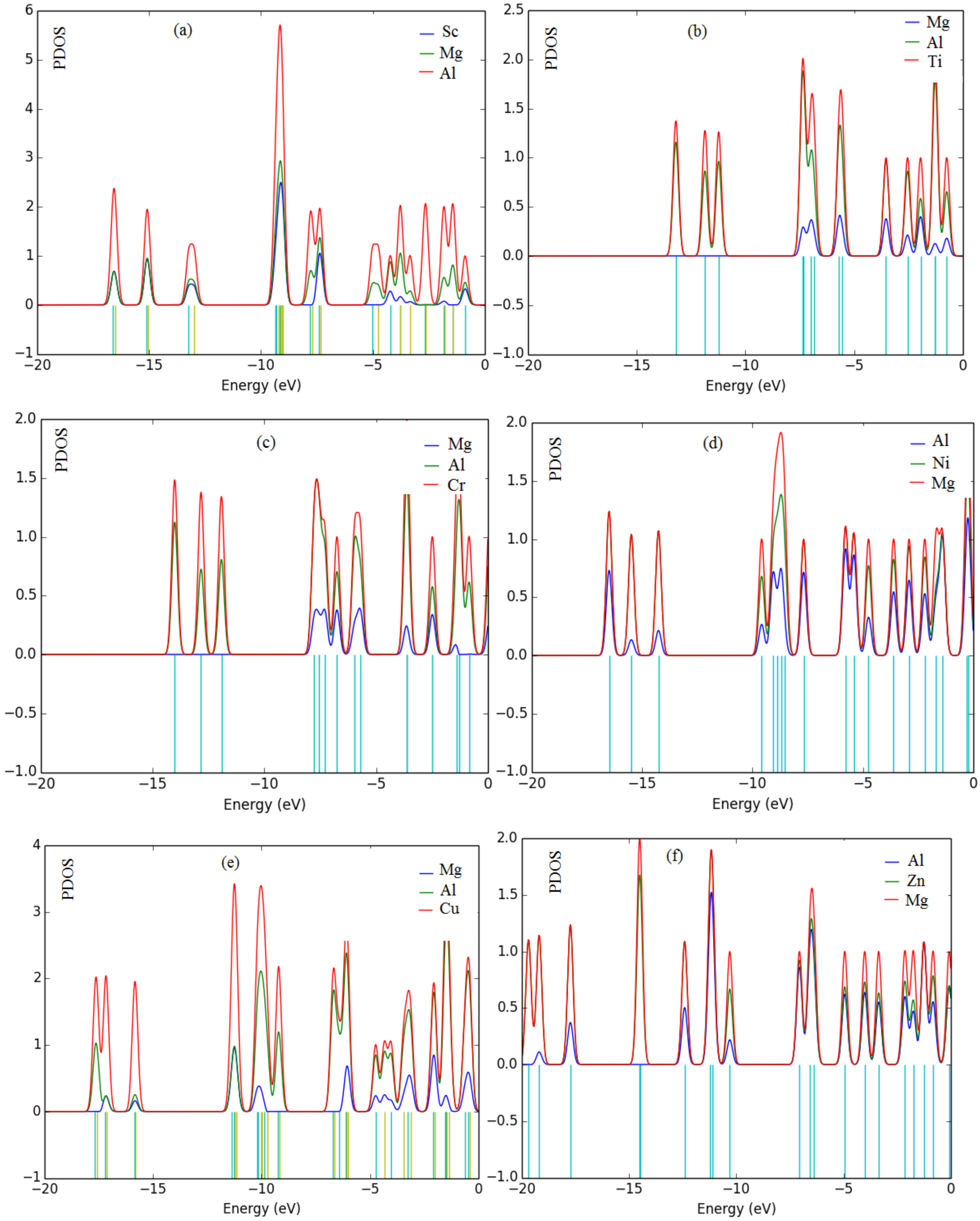

Figure3. "PDOS" adsorption of **a)** Sc–(Al–Mg), **b)** Ti–(Al–Mg), **c)** Cr–(Al–Mg), and **d)** Ni–(Al–Mg) , **e)** Cu–(Al–Mg) , and **f)** Zn–(Al–Mg) with Fermi level =0

Acta. Chim. Asiana., 2023, 6(2), 328 – 342

Table1. NMR properties of chemical shielding tensors (σ_{iso} & σ_{aniso}/ppm) and Bader atomic charge (Q/e) of transition metals attached in Py@TM–(Al–Mg), 2Pic→@TM–(Al–Mg),3Pic@TM–(Al–Mg), 4Pic@TM–(Al–Mg), and 24Lut@ TM–(Al–Mg) [TM= Sc, Ti, Cr, Ni, Cu, Zn] complexes.

Py@TM–(Al–Mg)						
ppm/e	Sc	Ti	Cr	Ni	Cu	Zn
σ_{iso}	1013.6918	503.5678	117.1780	514.5032	1724.3371	1335.1097
σ_{aniso}	763.9710	1342.6720	2818.4468	2614.0997	714.3705	810.1099
Q_{TM}	-5.7588	-3.6982	-2.7075	-1.5963	-1.3255	-1.4488
Q_N	-0.3740	-0.287	-2.7075	-1.5963	-0.5852	-0.5074
2Pic→@TM–(Al–Mg)						
ppm/e	Sc	Ti	Cr	Ni	Cu	Zn
σ_{iso}	926.5573	446.8853	1111.8100	823.7139	1641.1535	1413.3043
σ_{aniso}	685.0754	1525.1004	1379.9345	3768.6399	936.5758	1235.4950
Q_{TM}	-5.7898	-3.7283	-2.9442	-1.846052	-1.5752	-1.5474
Q_N	-0.2420	-0.2948	-0.3885	-0.405530	-0.4088	-0.3935
3Pic→@TM–(Al–Mg)						
ppm/e	Sc	Ti	Cr	Ni	Cu	Zn
σ_{iso}	1013.4773	636.8249	266.2060	759.9629	1708.9686	96.2601
σ_{aniso}	587.4224	2251.5198	2431.1067	1056.9293	758.0623	3417.9214
Q_{TM}	-5.7110	-3.618090	-2.7572	-1.7705	-1.3987	-1.4826
Q_N	-0.2588	-0.298569	-0.3993	-0.4359	-0.4491	-0.4165
4Pic→@TM–(Al–Mg)						
ppm/e	Sc	Ti	Cr	Ni	Cu	Zn
σ_{iso}	962.5782	670.5079	564.0696	387.4466	1698.3517	214.2436
σ_{aniso}	812.7171	1785.8061	1085.1472	2337.6286	469.5091	3294.1675
Q_{TM}	-5.8222	-3.7272	-2.8549	-1.7715	-1.4721	-1.5107
Q_N	-0.2729	-0.2926	-0.4023	-0.4386	-0.4450	-0.4080
24Lut@ TM–(Al–Mg)						
ppm/e	Sc	Ti	Cr	Ni	Cu	Zn
σ_{iso}	895.1995	915.7309	350.8908	583.5652	1875.1770	1638.1551
σ_{aniso}	216.0695	1119.3830	767.5820	3665.1157	737.6878	860.5583
Q_{TM}	-3.5596	-3.5596	-2.7038	-1.7769	-1.3865	-1.5156
Q_N	-0.2910	-0.2910	-0.4115	-0.4538	-0.4597	-0.4187

In Table 1, "NMR" data has reported the notable amounts for transition metals of "Sc, Ti, Cr, Ni, Cu, Zn" elements which have been doped on the AlMg surface through the adsorption of pyridine and alkylpyridines. In fact, the adsorption of pyridine and alkylpyridines of 2Pic, 3 Pic, 4 Pic and 24Lut molecules introduces spin polarization on the TM (Sc, Ti, Cr, Ni, Cu, Zn)-doped "AlMg" nanoalloy surfaces which indicates that these surfaces might be applied as magnetic nitrogen heterocycle detectors. In fact, it is revealed that the "isotropic" and "anisotropy" shielding augment with the occupancy and the negative Bader charge in pyridine and alkylpyridines penetrated by "N-atoms" in the benzene ring diffusing onto TM-doped AlMg surface. It has been exhibited that the atomic charge graph of "N-atom" has the same tendency, however a considerable deviation from transition metal elements (Figure4a-e).

In Figure4 (a-e), Sc, Ti, Cr, Ni, Cu, Zn in the complexes of Py@TM–(AlMg) (Figure4a), 2Pic→@TM–(AlMg) (Figure4b), 3Pic@TM–(AlMg) (Figure4c), 4Pic@TM–(AlMg) (Figure4d), and 24Lut@ TM–(AlMg) (Figure4e) denote the fluctuation in the atomic charge.

In fact, Figure4 (a-e) indicates that the gap Bader charge between nitrogen atom and transitions metals "TM" has the maximum value for "Sc", while has the minimum value for "Zn". On the other hand, it can be considered that the efficiency of electron accepting for the transition metals doped on the "AlMg" surface is "Zn> Cu > Ni > Cr > Ti > Sc" that indicates the power of covalent bond between nitrogen and transition metal.

Electrostatic properties & "NQR"

As the "EFG" at the citation of the nucleus in N-heterocycles is allocated by the valence electrons twisted in the particular attachment with close nuclei of TM-doped "AlMg" alloy crystal, the "NQR" frequency at which transitions occur is particular for an N-heterocycle @TM–(AlMg) complex (Table2). "NQR" is a straight frame of the interaction of the "quadrupole moment" with the "EFG" which is produced by the electronic structure of its ambiance [77-80].

Acta. Chim. Asiana., 2023, 6(2), 328 – 342

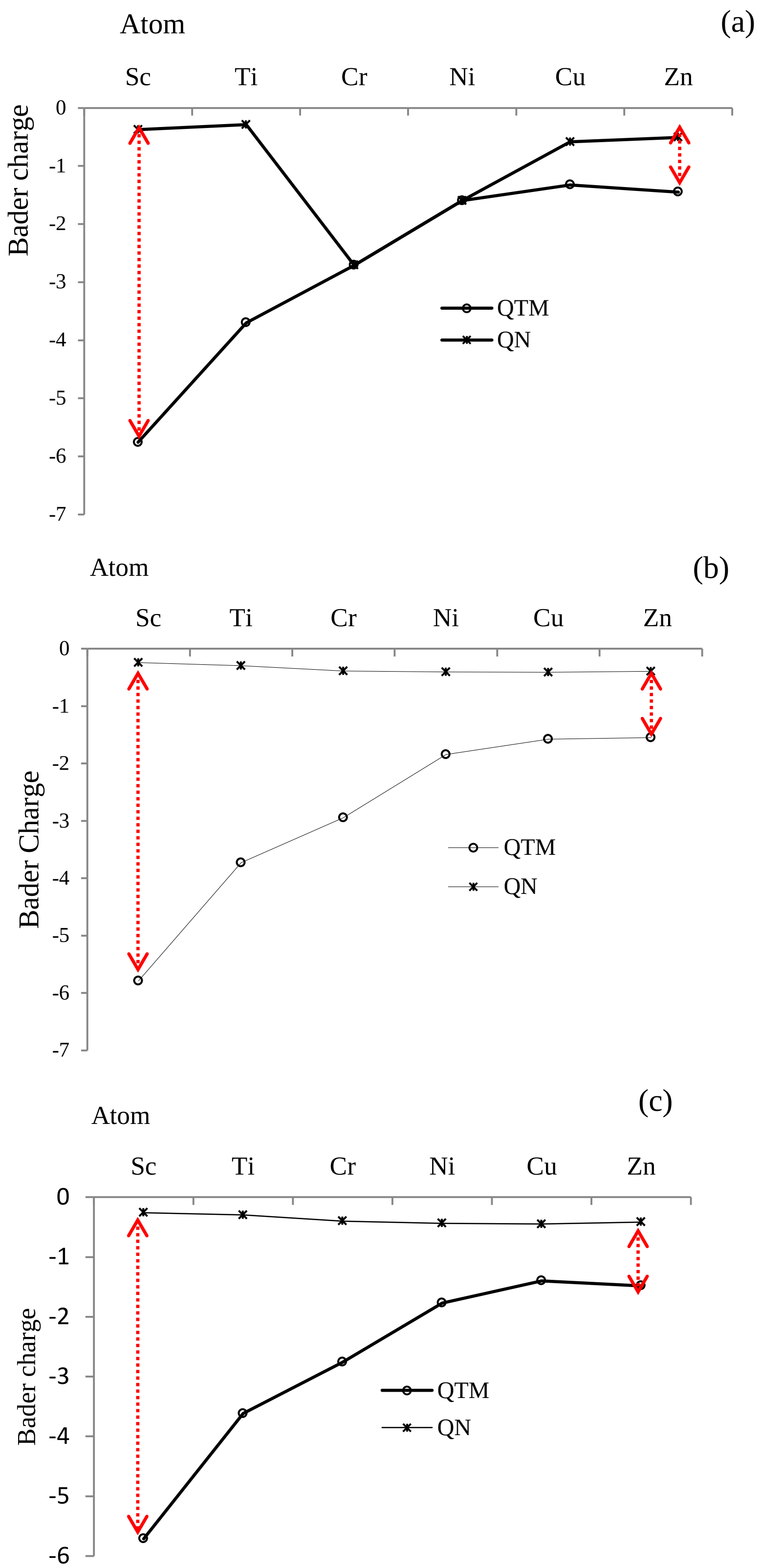

Acta. Chim. Asiana., 2023, 6(2), 328 – 342

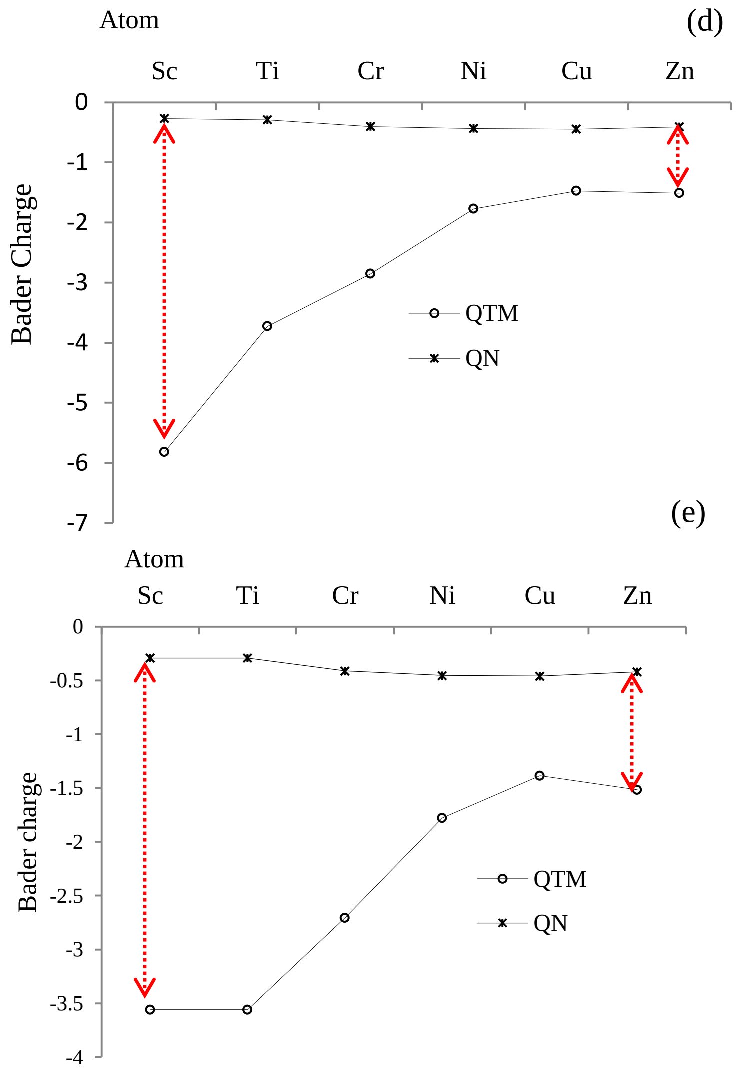

Figure4. The Bader charge for transition metal of "Sc, Ti, Cr, Ni, Cu, Zn" in the active site bound to N-atom of **a)** pyridine and alkylpyridines including **b)** 2-picoline (2Pic), **c)** 3-picoline (3Pic), **d)** 4-picoline (4Pic), and **e)** 2,4-lutidine (24Lut) through adsorption on the TM-doped Al–Mg alloy accompanying "CAM-B3LYP/EPR-III, LANL2DZ,6-31+G(d,p)"

In this research work, the "electric potential" as the quantity of work energy through carrying over the electric charge from one position to another position in the essence of electric field has been evaluated for Py@TM–(AlMg), 2Pic→@TM–(AlMg), 3Pic@TM–(AlMg), 4Pic@TM–(AlMg), and 24Lut@ TM–(AlMg) complexes using "CAM-B3LYP/EPR-III,LANL2DZ, 6-31+G(d,p)" level of theory (Table2).

Furthermore, in Figure5, it has been sketched the "electric potential" of nuclear quadrupole resonance for some atoms of nitrogen, aluminum, magnesium , scandium, titanium, nickel, chromium, copper and zinc in the adsorption process of pyridine and alkylpyridines on the TM-doped "AlMg" alloy surface which have been calculated by "CAM-B3LYP/EPR-III, 6-311+G (d,p), LANL2DZ".

In Figure 5, it has been described the influence of the replacement of aluminum metal elements in "AlMg" surface with "Sc, Ti, Cr, Ni, Cu, Zn". It’s vivid that the curve of "AlMg" is waved by these transition metals. The sharpest peaks for electric potential have been shown around transition metals doping of the AlMg which presents the electron accepting characteristics of these atoms versus the nitrogen atoms of heterocycles in pyridine and alkylpyridines (Figure5).

Acta. Chim. Asiana., 2023, 6(2), 328 – 342

Table2. The electric potential (a.u.) for elements of pyridine and alkylpyridines which have been adsorbed on the TM–(Al–Mg) alloy surface by CAM-B3LYP/EPR-III,6-31+G(d,p) calculation extracted of "NQR" method.

Py@TM–(AlMg)

Atom	Sc	Ti	Cr	Ni	Cu	Zn
N1	-18.0634	-18.0715	-18.0717	-18.0833	-18.0957	-18.078
Al7	-43.6667	-43.7526	-43.7366	-43.7434	-43.7427	-43.7466
Mg8	-38.6072	-38.7174	-38.7388	-38.7228	-38.7213	-38.7174
Al9	-43.5021	-43.5805	-43.5822	-43.59	-43.5818	-43.5914
Mg10	-38.845	-38.8997	-38.9028	-38.8886	-38.8898	-38.9004
Al11	-43.6826	-43.76	-43.767	-43.7806	-43.7853	-43.8095
Mg12	-38.5784	-38.6944	-38.7237	-38.6896	-38.7079	-38.723
TM13	-84.5456	-90.5066	-102.305	-126.941	-133.4	-139.905
Mg14	-38.571	-38.7102	-38.7417	-38.6752	-38.6717	-38.6623
Al15	-43.4504	-43.507	-43.5108	-43.5133	-43.5089	-43.5084
Al16	-43.4874	-43.5569	-43.5539	-43.5427	-43.5393	-43.5474
Mg17	-38.8307	-38.9015	-38.8924	-38.8988	-38.9012	-38.9077
Al18	-43.4774	-43.5663	-43.5485	-43.5402	-43.5674	-43.5521

2Pic@TM–(AlMg)

Atom	Sc	Ti	Cr	Ni	Cu	Zn
N1	-18.0834	-18.1051	-18.1293	-18.1542	-18.162	-18.1591
Al8	-43.6797	-43.7881	-43.7834	-43.7698	-43.7752	-43.7972
Mg9	-38.6185	-38.7308	-38.7691	-38.7442	-38.7455	-38.7511
Al10	-43.4179	-43.4664	-43.4637	-43.4491	-43.4536	-43.4523
Mg11	-38.8359	-38.8876	-38.8801	-38.8866	-38.8775	-38.8753
Al12	-43.682	-43.7583	-43.758	-43.7703	-43.7685	-43.7763
Mg13	-38.6233	-38.7378	-38.7812	-38.8019	-38.7764	-38.7803
TM14	-84.5483	-90.5223	-102.329	-127.002	-133.438	-139.943
Mg15	-38.5829	-38.7133	-38.7599	-38.7378	-38.7344	-38.716
Al16	-43.4674	-43.5279	-43.5217	-43.5401	-43.5387	-43.5325
Al17	-43.549	-43.6169	-43.6432	-43.6141	-43.6081	-43.6131
Mg18	-38.8742	-38.939	-38.9595	-38.9384	-38.9358	-38.951
Al19	-43.4413	-43.5034	-43.5103	-43.5222	-43.5267	-43.5262

3Pic@TM–(AlMg)

Atom	Sc	Ti	Cr	Ni	Cu	Zn
N1	-18.0635	-18.095	-18.1058	-18.1121	-18.1321	-18.136
Al8	-43.6782	-43.7491	-43.7449	-43.7751	-43.7609	-43.759
Mg9	-38.5886	-38.6938	-38.7335	-38.7588	-38.731	-38.732
Al10	-43.4991	-43.5564	-43.5605	-43.5267	-43.5204	-43.5516
Mg11	-38.8181	-38.8874	-38.9118	-38.9002	-38.8852	-38.8894
Al12	-43.663	-43.7533	-43.7187	-43.7258	-43.7418	-43.7612
Mg13	-38.6064	-38.7125	-38.7381	-38.7434	-38.7233	-38.7185
TM14	-84.5236	-90.4823	-102.288	-127	-133.411	-139.914
Mg15	-38.5637	-38.7017	-38.7449	-38.7028	-38.6787	-38.6766
Al16	-43.4383	-43.4929	-43.4939	-43.4975	-43.5015	-43.5128
Al17	-43.534	-43.6036	-43.6118	-43.6067	-43.5982	-43.5962
Mg18	-38.88	-38.9378	-38.9565	-38.953	-38.9498	-38.9783
Al19	-43.5196	-43.5775	-43.6072	-43.6254	-43.6015	-43.5994

4Pic@TM–(AlMg)

Atom	Sc	Ti	Cr	Ni	Cu	Zn
N1	-18.0687	-18.0913	-18.1079	-18.1227	-18.1306	-18.1184
Al8	-43.6682	-43.7745	-43.7528	-43.7564	-43.7673	-43.7872
Mg9	-38.6052	-38.7096	-38.7507	-38.7203	-38.7259	-38.7279
Al10	-43.491	-43.5512	-43.5506	-43.5441	-43.5415	-43.5332
Mg11	-38.8424	-38.9017	-38.8905	-38.9017	-38.8949	-38.8943
Al12	-43.6776	-43.7495	-43.7418	-43.7553	-43.7494	-43.7534
Mg13	-38.6145	-38.7221	-38.7609	-38.7708	-38.7504	-38.7556
TM14	-84.5401	-90.5062	-102.319	-126.991	-133.423	-139.927
Mg15	-38.5786	-38.7054	-38.7475	-38.7219	-38.7	-38.6873
Al16	-43.4824	-43.5505	-43.5365	-43.5678	-43.5555	-43.5461
Al17	-43.5354	-43.5921	-43.6093	-43.5907	-43.5798	-43.5842
Mg18	-38.8526	-38.9117	-38.928	-38.9121	-38.9105	-38.9255
Al19	-43.4344	-43.4978	-43.5049	-43.5185	-43.5098	-43.5066

24Lut@TM–(AlMg)

Atom	Sc	Ti	Cr	Ni	Cu	Zn
N1	-18.0689	-18.0776	-18.1001	-18.1155	-18.1168	-18.1048
Al9	-43.6482	-43.6966	-43.6771	-43.6947	-43.6889	-43.6875
Mg10	-38.5699	-38.6951	-38.7101	-38.7308	-38.7169	-38.7063
Al11	-43.5328	-43.6226	-43.6345	-43.6111	-43.6068	-43.6097
Mg12	-38.8455	-38.9299	-38.9284	-38.9514	-38.9418	-38.9344
Al13	-43.6482	-43.7189	-43.6818	-43.6881	-43.687	-43.6966
Mg14	-38.585	-38.6991	-38.7249	-38.7331	-38.706	-38.7031
TM15	-84.5081	-90.4727	-102.269	-126.976	-133.395	-139.903
Mg16	-38.5363	-38.6746	-38.7082	-38.6904	-38.654	-38.6444
Al17	-43.4858	-43.5504	-43.5511	-43.5519	-43.5479	-43.5863
Al18	-43.5258	-43.6095	-43.5873	-43.5971	-43.5895	-43.5763
Mg19	-38.88	-38.9741	-38.9832	-38.975	-38.9561	-38.9719
Al20	-43.506	-43.6099	-43.6229	-43.6066	-43.6127	-43.6151

Acta. Chim. Asiana., 2023, 6(2), 328 – 342

Table3. The Physicochemical properties of adsorption for Py@TM–(AlMg), 2Pic→@TM–(AlMg), 3Pic@TM–(AlMg), 4Pic@TM–(AlMg), and 24Lut@ TM–(AlMg) complexes as corrosion inhibitors of N-heterocyclic carbenes and TM–(AlMg) alloy surface (TM= Sc, Ti, Cr, Ni, Cu, and Zn).

Compound	$\Delta E^o \times 10^{-4}$ (kcal/mol)	$\Delta H^o \times 10^{-4}$ (kcal/mol)	$\Delta G^o \times 10^{-4}$ (kcal/mol)	S^o (cal/K.mol)	Dipole moment (Debye)
AlMg	-166.2904	-166.2904	-166.2926	75.228	0.3215
Sc–(AlMg)	-198.3723	-198.3722	-198.3745	75.375	0.5659
Ti–(AlMg)	-203.9286	-203.9285	-203.9308	76.021	0.6583
Cr–(AlMg)	-216.0621	-216.0621	-216.0643	75.667	1.7628
Ni–(AlMg)	-244.8328	-244.8328	-244.8350	74.120	0.0800
Cu–(AlMg)	-253.0143	-253.0142	-253.0166	79.123	0.0682
Zn–(AlMg)	-261.6103	-261.6102	-261.6125	75.871	0.3346
Pyridine	-15.3793	-15.3792	-15.3813	68.627	2.0338
Py@AlMg	-181.6098	-181.6094	-181.6094	88.026	2.7271
Py@Sc–(AlMg)	-213.6747	-213.6746	-213.6772	88.194	1.4862
Py@Ti–(AlMg)	-219.2404	-219.2403	-219.2428	83.855	1.1762
Py@Cr–(AlMg)	-231.3740	-231.3739	-231.3765	84.265	3.1318
Py@Ni–(AlMg)	-260.1413	-260.1412	-260.1437	82.198	0.8350
Py@Cu–(AlMg)	-268.3194	-268.3194	-268.3219	86.730	1.0624
Py@Zn–(AlMg)	-276.9130	-276.9129	-276.9155	85.142	2.6477
2Pic	-17.8155	-17.8154	-17.8176	73.692	1.7413
2Pic @AlMg	-184.0349	-184.0348	-184.0375	90.184	2.9225
2Pic @Sc–(AlMg)	-216.1087	-216.1087	-216.1112	86.878	2.8023
2Pic @Ti–(AlMg)	-221.6693	-221.6692	-221.6717	84.761	1.5756
2Pic @Cr–(AlMg)	-233.8027	-233.8026	-233.8052	88.166	2.5826
2Pic @Ni–(AlMg)	-262.5686	-262.5686	-262.5711	84.840	2.3451
2Pic @Cu–(AlMg)	-270.7476	-270.7475	-270.7501	86.487	2.1705
2Pic @Zn–(AlMg)	-279.3410	-279.3410	-279.3436	89.798	2.6052
3Pic	-17.8154	-17.8153	-17.8175	73.725	2.2156
3Pic @Al–Mg	-184.0555	-184.0554	-184.0580	87.228	3.7142
3Pic @Sc–(AlMg)	-216.1270	-216.1270	-216.1295	85.732	1.7486
3Pic @Ti–(AlMg)	-221.6897	-221.6897	-221.6923	87.063	1.5275
3Pic @Cr–(AlMg)	-233.8218	-233.8217	-233.8244	88.565	2.7098
3Pic @Ni–(AlMg)	-262.5884	-262.5884	-262.5911	90.691	1.1313
3Pic @Cu–(AlMg)	-270.7672	-270.7672	-270.7699	91.911	1.6406
3Pic @Zn–(AlMg)	-279.3604	-279.3604	-279.3630	88.744	2.7259
4Pic	-17.8154	-17.8154	-17.8176	73.717	2.4672
4Pic @AlMg	-184.0535	-184.0534	-184.0559	84.850	2.4644
4Pic @Sc–(AlMg)	-216.1239	-216.1238	-216.1263	83.858	2.0253
4Pic @Ti–(AlMg)	-221.6866	-221.6866	-221.6891	86.720	1.3866
4Pic @Cr–(AlMg)	-233.8190	-233.8190	-233.8216	88.096	2.0330
4Pic @Ni–(AlMg)	-262.5867	-262.5866	-262.5892	87.216	0.8754
4Pic @Cu–(AlMg)	-270.7651	-270.7650	-270.7676	88.196	1.0307
4Pic @Zn–(AlMg)	-279.3583	-279.3583	-279.3608	85.564	2.3789
24Lut	-20.2516	-20.2515	-20.2539	78.728	2.1610
24Lut @AlMg	-186.5020	-186.5020	-186.5048	93.257	3.0400
24Lut @Sc–(AlMg)	-218.5703	-218.5703	-218.5730	92.005	1.5329
24Lut @Ti–(AlMg)	-224.1338	-224.1337	-224.1364	90.600	0.7545
24Lut @Cr–(AlMg)	-236.2646	-236.2645	-236.2673	92.253	3.0715
24Lut @Ni–(AlMg)	-265.0321	-265.0320	-265.0348	91.590	1.2308
24Lut @Cu–(AlMg)	-273.2115	-273.2114	-273.2141	91.324	1.4305
24Lut @Zn–(AlMg)	-281.8061	-281.8060	-281.8088	92.247	3.5104

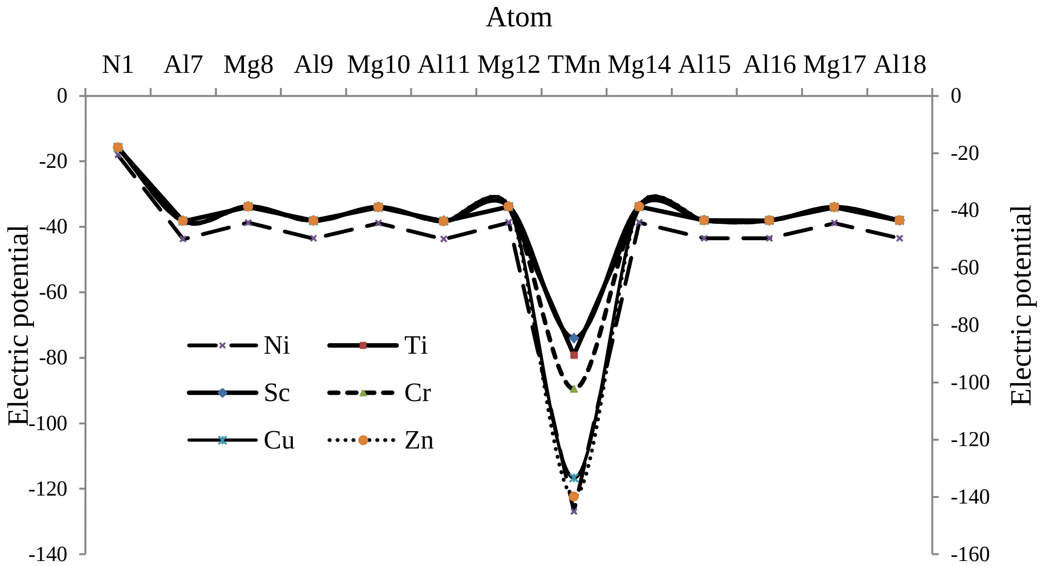

Figure5. "Electric potential" (a.u.) versus "atomic charge" (e) through "NQR" calculation for pyridine and alkylpyridines on the (Sc, Ti, Cr, Ni, Cu, Zn)-doped AlMg alloy surface by "CAM-B3LYP/EPR-III, LANL2DZ,6-31+G(d,p)".

"IR" spectroscopy & thermodynamic analysis

The "IR" calculations have been accomplished for adsorption of five N-heterocyclic inhibitor carbenes of pyridine and alkylpyridines containing 2Pic, 3Pic, 4Pic and 24Lut on the TM (Sc, Ti, Cr, Ni, Cu, and Zn)-doped Al–Mg alloy surface. Therefore, it has been simulated the several clusters containing Py@TM–(AlMg), 2Pic→@TM–(AlMg), 3Pic@TM–(AlMg), 4Pic@TM–(AlMg), and 24Lut@ TM–(AlMg) (Table3). These materials have been accounted at "CAM-B3LYP" level of theory accompanying "6-31+ G (d,p) /EPRIII /LANL2DZ" basis sets to receive the more valid equilibrium geometrical specifications, physical and thermodynamic parameter for each of the dedicated composition. (Table 3).

Based on Table 3, the thermodynamic specifications, the authors concluded that this protective film containing the (Pyridine & alkylpyridines)@ TM–(AlMg) complexes which might be effective through doping of transition metals (TM) of "Sc, Ti, Cr, Ni, Cu, Zn" including Py@TM–(AlMg), 2Pic@TM–(AlMg), 3Pic@TM–(AlMg), 4Pic@TM–(AlMg), and 24Lut@TM–(AlMg).

The "adsorptive capacity" of pyridine and alkylpyridines on the "TM–(AlMg)" (TM= Sc, Ti, Cr, Ni, Cu, Zn) surface is affirmed by the ΔG^{o}_{ads} quantities:

$$\Delta G^{o}_{ads} = \Delta G^{o}_{adsorate@TM-(Al-Mg)} - \left(\Delta G^{o}_{adsorbate} + \Delta G^{o}_{TM-(Al-Mg)}\right)\ ;\ X = \mathrm{Sc, Ti, Cr, Ni, Cu, Zn} \qquad (15)$$

Remarking Table3, it is discovered that the adsorbing process of the N-heterocyclic carbenes on the "TM–(AlMg)" alloy might be physical and chemical nature. As seen in Table3, all the accounted ΔG^{o}_{ads}amounts are very close, which demonstrate the agreement of the measured specifications by all methodologies and the reliability of the computing values.

CONCLUSIONS

This study has analyzed the molecular properties of AlMg and the difference in its properties when doped with Transition metals "TM" of "Sc, Ti, Cr, Ni, Cu, and Zn". Denoting this research, the efficiency of the "N-heterocyclic carbenes" as the inhibiting agents for TM–(AlMg) has been investigated through the electromagnetic and thermochemical thermoelectric traits extracts from "PDOS", "NMR", "NQR", "IR" analysis which have been performed on Py@TM–(AlMg), 2Pic→@TM–(AlMg), 3Pic@TM–(AlMg), 4Pic@TM–(AlMg), and 24Lut@ TM–(AlMg).

In the preferred path, the these N-heterocyclic carbenes of pyridine and alkylpyridines stay collateral to the plane so long as fulfilling small single rotational steps with a "C–C" double bond belonged above a single transition metal element in "TM–(AlMg)" nanoalloy. The inhibiting process of the protonated pyridine and alkylpyridines compositions is quoted to the total of the pure charge and the "π charge "of the "six-ring". Pyridine and alkylpyridines have been adsorbed on the crystal surface of the "TM–(AlMg)" electrodes primarily in their protonated shapes.

Acknowledgments: In successfully completing this paper and its research, the authors are grateful to "Kastamonu University" for their support through the library, the laboratory, and scientific websites.

REFERENCES

[1 Ahmad, Z., 2006. Principles of Corrosion Engineering and Corrosion Control. Elsevier Science and Technology Books.
2. Wei, C. Electrochemical deposition of aluminum. Technol. Innov. Appl. 2019, 18, 80-81.
3. Yang, H.M.; Qiu, Z.X.; Zhang, G. Low Temperature Aluminum Electrolysis; Northeast University Press: Shenyang, China, 2009.
4. Lu, H.M.; Qiu, Z.X. Research progress of low temperature aluminum electrolysis. Light Metals 1997, 4, 24.
5. Machnikova E, Whitmire KH, Hackerman N. Corrosion inhibition of carbon steel in hydrochloric acid by furan derivatives. Electrochim. Acta, 2008; 53: 6024–6032. DOI:10.1016/j.electacta.2008.03.021.
6. Benabdellah M, Touzani R, Aouniti A, et alInhibitive action of some bipyrazolic compounds on the corrosion of steel in 1 M HCl: Part I: Electrochemical study. Mater. Chem. Phys., 2007; 105: 373–379. DOI:10.1016/j.matchemphys.2007.05.001.
7. Fiala,A, Chibani A, Darchen A, et al. Investigations of the inhibition of copper corrosion in nitric acid solutions by ketene dithioacetal derivatives. Appl. Surf. Sci., 2007; 253: 9347–9356. DOI:10.1016/j.apsusc.2007.05.066.
8. Prabhu RA, Shanbhag AV, Venkatesha TV. Influence of tramadol [2-[(dimethylamino) methyl]-1-(3-methoxyphenyl) cyclohexanol hydrate] on corrosion inhibition of mild steel in acidic media. J Appl Electrochem 2007; 37: 491–497. DOI: 10.1007/s10800-006-9280-2.
9. Tian, G.C.; Li, J.; Hua, Y.X. Application of ionic liquids in metallurgy of nonferrous metals. Chin. J. Process Eng. 2009, 9, 200.
10. Tian, G.C.; Li, J.; Hua, Y.X. Application of ionic liquids in hydrometallurgy of nonferrous metals. Trans. Nonferrous Met. Soc. China 2010, 20, 513.
11. Monajjemi, M.; Afsharnezhad, S.; Jaafari, M.R.; Mirdamadi, S.; Mollaamin, F.; Monajemi, H. Investigation of energy and NMR isotropic shift on the internal rotation Barrier of Θ4 dihedral angle of the DLPC: A GIAO study. Chemistry 2008, 17, 55-69.
12. Tian, G.C. Ionic liquids as green electrolytes for Aluminum and Aluminum-alloy production. Mater. Res. Found. 2019, 54, 249.
13. Zhong, X.W.; Xiong, T.; Lu, J.; **339** Advances of electro-deposition and refining of aluminum and aluminum al liquid electrolytes system. Nonferrous Met. Sci. Eng. 2014, 5, 44.
14. Zheng, Y.; Wang, Q.; Zheng, Y.J.; Lv, H.C. Advances in research and application of aluminum electrolysis in ionic liquid systems. Chin. J. Process Eng. 2015, 15, 713.
15. Fleury, V.; Kaufman, J.H.; Hibbert, D.B. Mechanism of a morphology transition in ramified electrochemical growth. Nature 1994, 367, 435.
16. Yue, G.; Lu, X.; Zhu, Y.; Zhang, X.; Zhang, S. Surface morphology, crystal structure and orientation of aluminum coatings electrodeposited on mild steel in ionic liquid. Chem. Eng. J. 2009, 147, 79.
17. Barth, J. V.; Brune, H.; Ertl, G.; Behm, R. J. Scanning tunneling microscopy observations on the reconstructed Au(111) surface: Atomic structure, long-range superstructure, rotational domains, and surface defects. Phys. Rev. B. 1990, 42, 9307-9318.
18. Esken, D.; Turner, S.; Lebedev, O. I.; van Tendeloo, G.; Fischer, R. A. Au@ ZIFs: stabilization and encapsulation of cavity-size matching gold clusters inside functionalized zeolite imidazolate frameworks, ZIFs. Chem. Mater. 2010, 22, 6393-6401.
19. Mollaamin, F.; Monajjemi, M. Fractal Dimension on Carbon Nanotube-Polymer Composite Materials Using Percolation Theory. Journal of Computational and Theoretical Nanoscience 2012, 9, 597-601, https://doi.org/10.1166/jctn.2012.2067.
20. Liu, B.; Smit, B. Molecular Simulation Studies of Separation of CO2/N2, CO2/CH4, and CH4/N2 by ZIFs. J. Phys. Chem. C, 2010, 114, 8515-8522.
21. Keskin, S. Atomistic Simulations for Adsorption, Diffusion, and Separation of Gas Mixtures in Zeolite Imidazolate Frameworks. J. Phys. Chem. C, 2010, 115, 800-807.
22. Tran, U. P. N.; Le, K. K. A.; Phan, N. T. S. Expanding applications of metal- organic frameworks: zeolite imidazolate framework ZIF-8 as an efficient heterogeneous catalyst for the knoevenagel reaction. ACS Catal., 2011, 1, 120-127.
23. VandeVondele, J.; Krack, M.; Mohamed, F.; Parrinello, M.; Chassaing, T.; Hutter, J. Quickstep: Fast and accurate density functional calculations using a mixed Gaussian and plane waves approach. Comp. Phys. Comm., 2005, 2, 103-128.
24. Phan, A.; Doonan, C. J.; Uribe-Romo, F. J.; Knobler, C. B.; O'keeffe, M.; Yaghi, O. M. Synthesis, structure, and carbon dioxide capture properties of zeolitic imidazolate frameworks. Acc. Chem. Res., 2010, 43, 58-67.
25. Hohenberg, P.; Kohn, W. Inhomogeneous Electron Gas. Phys. Rev. B, 1964, 136, B864-B871.
26. Kohn, W.; Sham, L. J. Self-Consistent Equations Including Exchange and Correlation Effects.Phys. Rev., 1965, 140, A1133- A1138.

27. Lippert, G.; Hutter, J.; Parrinello, M. A hybrid Gaussian and plane wave density functional scheme. Mol. Phys., 1997, 92, 477-487.
28. Hartwigsen, C.; Goedecker, S.; Hutter, J. Relativistic separable dual-space Gaussian pseudopotentials from H to Rn. Phys. Rev. B, 1998, 58, 3641-3662.
29. Perdew, J. P.; Burke, K.; Ernzerhof, M. Generalized Gradient Approximation Made Simple.Phys. Rev. Lett., 1996, 77, 3865-3868.
30. VandeVondele, J.; Hutter, J. Gaussian basis sets for accurate calculations on molecular systems in gas and condensed phases. J. Chem. Phys., 2007, 127, 114105-1_114105-9.
31. Monajjemi, M.; Mahdavian, L.; Mollaamin, F. Characterization of nanocrystalline silicon germanium film and nanotube in adsorption gas by Monte Carlo and Langevin dynamic simulation. Bulletin of the Chemical Society of Ethiopia 2008, 22, 277-286, https://doi.org/10.4314/bcse.v22i2.61299.
32. Mavrikakis, M.; Stoltze, P.; Nørskov, J. K. Making gold less noble. Catal. Lett., 2000, 64, 101-106.
33. Dal Corso, A.; Ab initio phonon dispersions of transition and noble metals: effects of the exchange and correlation functional. J. Phys.; Condens. Matter, 2013, 25, 145401-145410.
34. Whitman, L. J.; Stroscio, J. A.; Dragoset, R. A.; Celotta, R. J. Geometric and electronic properties of Cs structures on III-V (110) surfaces: From 1D and 2D insulators to 3D metals. Phys. Rev. Lett., 1991, 66, 1338-1341.
35. Mollaamin, F.; Baei, M.T.; Monajjemi, M.; Zhiani, R.; Honarparvar, B. A DFT study of hydrogen chemisorption on V (100) surfaces. Russian Journal of Physical Chemistry A, Focus on Chemistry 2008, 82, 2354-2361, https://doi.org/10.1134/S0036024408130323.
36. Yildirim, H.; Greber, T.; Kara, A. Trends in Adsorption Characteristics of Benzene on Transition Metal Surfaces: Role of Surface Chemistry and van der Waals Interactions. J. Phys. Chem. C, 2013, 117, 20572-20583.
37. Monajjemi, M.; Baie, M.T.; Mollaamin, F. Interaction between threonine and cadmium cation in [Cd(Thr)] (n = 1-3) complexes: Density functional calculations , Russian Chemical Bulletin , 2010, 59. 886-889, https://doi.org/10.1007/s11172-010-0181-5.
38. Hoefling, M.; Iori, F.; Corni, S.; Gottschalk, K. E. The Conformations of Amino Acids on a Gold(111) Surface. ChemPhysChem., 2010, 11, 1763-1767.
39. Bakhshi, K.; Mollaamin, F.; Monajjemi, M. Exchange and Correlation Effect of Hydrogen Chemisorption on Nano V(100) Surface: A DFT Study by Generalized Gradient Approximation (GGA). Journal of Computational and Theoretical Nanoscience 2011, 8, 763-768, https://doi.org/10.1166/jctn.2011.1750.
40. Valencia, H.; Kohyama, M.; Tanaka, S.; Matsumoto, H. Ab initio study of EMIM-BF4 crystal interaction with a Li (100) surface as a model for ionic liquid/Li interfaces in Li-ion batteries. J. Chem. Phys. 2009, 131, 244705.
41. Clarke-Hannaford, J.; Breedon, M.; Best, A.S.; Spencer, M.J. The interaction of ethylammoniumtetrafluoroborate [EtNH3+][BF4−] ionic liquid on the Li (001) surface, towards understanding early SEI formation on Li metal. Phys. Chem. Chem. Phys. 2019, 21, 10028–10037.
42. Zhang, Q.Q. Study on Electrodeposition of Aluminum and Aluminum Alloy in Ionic Liquid; University of Chinese Academy of Sciences: Beijing, China, 2014.
43. Mollaamin, F.; Monajjemi, M. Harmonic Linear Combination and Normal Mode Analysis of Semiconductor Nanotubes Vibrations. J. Comput. Theor. Nanosci 2015, 12, 1030-1039. doi:10.1166/jctn.2015.3846.
44. Ali SA, Mazumder MAJ, Nazal MK, Al-Muallem HA. 2020 Assembly of succinic acid and isoxazolidine motifs in a single entity to mitigate CO2 corrosion of mild steel in saline media. Arab. J. Chem. 13, 242–257. (doi:10. 1016/j.arabjc.2017.04.005)
45. Amar H, Benzakour J, Derja A, Villemin D, Moreau B. 2003 A corrosion inhibition study of iron by phosphonic acids in sodium chloride solution. J. Electroanal. Chem. 558, 131–139. (doi:10.1016/S0022-0728(03)00388-7)
46. El-Sayed MS. 2011 Corrosion and corrosion inhibition of aluminum in Arabian Gulf seawater and sodium chloride solutions by 3-amino-5-mercapto-1,2,4-triazole. Int. J. Electrochem. Sci. 6, 1479–1492.
47. Sherif ES. 2014 A comparative study on the electrochemical corrosion behavior of iron and X-65 steel in 4.0 wt % sodium chloride solution after different exposure intervals. Molecules 19, 9962–9974. (doi:10.3390/ molecules19079962)
48. Yang D, Zhang M, Zheng J, Castaneda H. 2015 Corrosion inhibition of mild steel by an imidazolium ionic liquid compound: the effect of pH and surface pre-corrosion. RSC Adv. 5, 95 160–95 170. (doi:10.1039/ C5RA14556B).
49. Finšgar, M.; Milošev I. (11 March 2010). "Inhibition of copper corrosion by 1,2,3-benzotriazole: A review". Corrosion Science. 52 (9): 2737–2749. doi:10.1016/j.corsci.2010.05.002
50. Shen, A. Y.; Wu, S. N.; Chiu, C. T. (1999). "Synthesis and Cytotoxicity Evaluation of some 8-Hydroxyquinoline Derivatives". Journal of Pharmacy and Pharmacology. 51 (5): 543–548. doi:10.1211/0022357991772826.
51. CABASSI, PAJ; et al. (November–December 1983). "The improved flotation of gold from the

residues of Orange Free State ores" (PDF). Journal of the South African Institute of Mining and Metallurgy. 83 (11): 270–276.

52. Monajjemi M, Mollaamin F, Gholami MR, et al. Quantum Chemical Parameters of Some Organic Corrosion Inhibitors, Pyridine, 2-Picoline 4-Picoline and 2, 4- Lutidine, Adsorption at Aluminum Surface in Hydrocholoric and Nitric Acids and Comparison Between Two Acidic Media. Main Group Met. Chem. 2003; 26: 349-362. https://doi.org/10.1515/MGMC.2003.26.6.349.
53. Mollaamin, F., Shahriari, S., Monajjemi, M. et al. Nanocluster of Aluminum Lattice via Organic Inhibitors Coating: A Study of Freundlich Adsorption. J Clust Sci 34, 1547–1562 (2023). https://doi.org/10.1007/s10876-022-02335-1
54. Mollaamin, F., Monajjemi, M. Corrosion Inhibiting by Some Organic Heterocyclic Inhibitors Through Langmuir Adsorption Mechanism on the Al-X (X = Mg/Ga/Si) Alloy Surface: A Study of Quantum Three-Layer Method of CAM-DFT/ONIOM. J Bio Tribo Corros 9, 33 (2023). https://doi.org/10.1007/s40735-023-00751-y.
55. Mollaamin F and Monajjemi M. Molecular modelling framework of metal-organic clusters for conserving surfaces: Langmuir sorption through the TD-DFT/ONIOM approach. MOLECULAR SIMULATION 2023; 49(4): 365–376. https://doi.org/10.1080/08927022.2022.2159996.
56. Mollaamin, F., Monajjemi, M. In Silico-DFT Investigation of Nanocluster Alloys of Al-(Mg, Ge, Sn) Coated by Nitrogen Heterocyclic Carbenes as Corrosion Inhibitors. J Clust Sci (2023). https://doi.org/10.1007/s10876-023-02436-5.
57. Zupanič, F.; Žist, S.; Albu, M.; Letofsky-Papst, I.; Burja, J.; Vončina, M.; Bončina, T. Dispersoids in Al-Mg-Si Alloy AA 6086 Modified by Sc and Y. Materials 2023, 16, 2949. https://doi.org/10.3390/ma16082949.
58. Li, S.; Dong, H.; Wang, X.; Liu, Z. Quenching Sensitivity of Al-Zn-Mg Alloy after Non-Isothermal Heat Treatment. Materials 2019, 12, 1595. https://doi.org/10.3390/ma12101595.
59. Wang, Z.; Zhang, P.; Zhao, X.; Rao, S. The Corrosion Behavior of Al-Cu-Li Alloy in NaCl Solution. Coatings 2022, 12, 1899. https://doi.org/10.3390/coatings12121899.
60. Svensson,M.; Humbel,S.; Froese,R.D.J.; Matsubara,T.; Sieber,S.; and Morokuma,K. ONIOM: A Multilayered Integrated MO + MM Method for Geometry Optimizations and Single Point Energy Predictions. A Test for Diels−Alder Reactions and Pt(P(t-Bu)3)2 + H2 Oxidative Addition. J. Phys. Chem. 1996, 100(50) , 19357–19363. https://doi.org/10.1021/jp962071j.
61. Ming-Dao,L., Lu-An, Y.,Qing-Yu, W., Xiao-Ci ,Y., Xiao-Dong, Y.,Jin-Yun, Z.,J.of Chinese Society of Corrosion and Protection.1996;16:3:195.
62. Sokkar, P.; Boulanger, E.; Thiel, W.; Sanchez-Garcia, E. J. Chem. 63. Theory Comput. 2015, DOI: 10.1021/ct500956u.
63. Felix Brandt, Christoph R. Jacob. Systematic QM Region Construction in QM/MM Calculations Based on Uncertainty Quantification. Journal of Chemical Theory and Computation 2022, 18 (4), 2584-2596. https://doi.org/10.1021/acs.jctc.1c01093.
64. Blöchl, P.E. Projector augmented-wave method. Phys. Rev. B 1994, 50, 17953–17979.
65. Perdew, J.P.; Burke, K.; Ernzerhof, M. Generalized gradient approximation made simple. Phys. Rev. Lett. 1996, 77, 3865.
66. Ziesche, P.; Kurth, S.; Perdew, J.P. Density functionals from LDA to GGA. Comput. Mater. Sci. 1998, 11, 122–127.
67. Arrigoni, M.; Madsen, G.K.H. Comparing the performance of LDA and GGA functionals in predicting the T lattice thermal conductivity of III-V semiconductor materials in the zincblende structure: The cases of AlAs and BAs. Comput. Mater. Sci. 2019, 156, 354–360.
68. Becke AD (1993) Density-functional thermochemistry. III. The role of exact exchange. J Chem Phys 98:5648–5652.
69. Lee C, Yang W, Parr RG (1988) Development of the Colle–Salvetti correlation-energy formula into a functional of the electron density. Phys Rev B 37:785–789.
70. K. Kim; K. D. Jordan (1994). "Comparison of Density Functional and MP2 Calculations on the Water Monomer and Dimer". J. Phys. Chem. 98 (40): 10089–10094. doi:10.1021/j100091a024.
71. P. J. Stephens; F. J. Devlin; C. F. Chabalowski; M. J. Frisch (1994). "Ab Initio Calculation of Vibrational Absorption and Circular Dichroism Spectra Using Density Functional Force Fields". J. Phys. Chem. 98 (45): 11623–11627. doi:10.1021/j100096a001.
72. C. J. Cramer (2004). "Essentials of Computational Chemistry: Theories and Models, 2nd Edition Wiley". Wiley.com. Retrieved 2021-06-24.
73. S. H. Vosko; L. Wilk; M. Nusair (1980). "Accurate spin-dependent electron liquid correlation energies for local spin density calculations: a critical analysis". Can. J. Phys. 58 (8): 1200–1211. Bibcode:1980CaJPh..58.1200V. doi:10.1139/p80-159.
74. Frisch, M. J.; Trucks, G. W.; Schlegel, H. B.; Scuseria, G. E.; Robb, M. A.; Cheeseman, J. R.; Scalmani, G.; Barone, V.; Petersson, G. A.; Nakatsuji, H.; et al. Gaussian 16, Revision C.01, Gaussian, Inc., Wallingford CT, 2016.
75. GaussView, Version 6.06.16, Dennington, Roy; Keith, Todd A.; Millam, John M. Semichem Inc., Shawnee Mission, KS, 2016.
76. Sohail, U.; Ullah, F.; Binti Zainal Arfan, N.H.; Abdul Hamid, M.H.S.; Mahmood, T.; Sheikh,

N.S.; Ayub, K. Transition Metal Sensing with Nitrogenated Holey Graphene: A First-Principles Investigation. Molecules 2023, 28, 4060. https://doi.org/10.3390/molecules28104060.
77. Smith, J. A. S. (January 1971). "Nuclear Quadrupole Resonance Spectroscopy". Journal of Chemical Education. 48: 39–41.
78. Appendix K: Nuclear quadrupole resonance, by Allen N. Garroway, Naval Research Laboratory. In Jacqueline MacDonald, J. R. Lockwood: Alternatives for Landmine Detection. Report MR-1608, Rand Corporation, 2003.
79. O. Kh. Poleshchuck, E.L. Kalinna, J. N. Latosinska, J. Koput, Journal of Molecular Structure (Theochem) 547 (2001) 233 – 243.
80. Young, Hugh A.; Freedman, Roger D. (2012). Sears and Zemansky's University Physics with Modern Physics (13th ed.). Boston: Addison-Wesley. p. 754.